Progress In Electromagnetics Research C, Vol. 37, 95–106, 2013

DUAL-BAND BANDPASS FILTER USING A SINGLE SHORT-ENDED DUAL-MODE RESONATOR WITH ADJUSTABLE FIRST PASSBAND

Shoujia Sun*, Shuai Yang, Bian Wu, Kun Deng, and Changhong Liang

National Key Laboratory of Antennas and Microwave Technology, Xidian University, Xi'an 710071, P. R. China

Abstract—In this paper, a novel dual-band bandpass filter (BPF) based on a single short-ended dual-mode resonator (SEDMR) is presented. According to the voltage distribution of the resonator, two pairs of loaded open stubs, inside and outside of the resonator, are utilized to tune the center frequency and the external quality factor of the first passband respectively, while there is no influence on the second passband. Meanwhile, source-load coupling is introduced to produce transmission zeros to improve the passband selectivity and band-to-band isolation. For demonstration, a dual-band filter working at 1.52 GHz for GPS and 3.5 GHz for WiMax is designed, fabricated and measured with insertion losses of 1.47 and 0.95 dB. In addition, two transmission zeros, introduced by source-load coupling, located at 2.19 and 2.67 GHz between the first and second passband improve passband selectivity and band-to-band isolation better than 50 dB.

1. INTRODUCTION

To meet the requirement in the recent development of advanced multi-band wireless system, the dual-band BPF [1] becomes a good candidate. Therefore, it is highly desirable to develop various dual-band BPFs. Since the concept of microstrip dual-mode BPF was presented by Wolff [2], the dual-band filters based on the dual-mode resonator have been attracting much more attention in recent years due to their compact size and good roll-off skirt.

So far, several main ways to design dual-band filter are summarized as follows. First, two sets of resonators with different

Received 1 January 2013, Accepted 30 January 2013, Scheduled 31 January 2013

* Corresponding author: Shoujia Sun (sunshoujia@gmail.com).

resonant frequencies are employed to form dual-band response, which needs at least four resonators and leads to a large circuit size [3–5]; Second, a dual-band filter can be achieved by cascading the stepped impedance resonator (SIR) or stub loaded resonator (SLR), and two resonators at least are required [6–12]; Last, for a compact circuit size, the dual-mode resonator becomes an important candidate and is arranged for dual-band application, which needs at least one or two resonators. In [13–16], two dual-mode resonators with different sizes are properly formed in a single- or two-layer substrate to realize dual-band filter with compact size, low insertion loss and high selectivity. However, there are little reports on dual-mode dual-band filter using only one single resonator [17–21]. In this case, it will attract more and more attention due to its more compact size.

This paper presents a novel dual-band BPF based on a single short-ended dual-mode resonator (SEDMR), which has been proposed and utilized to design wideband bandpass filters by the author in [22]. In this paper, the SEDMR is employed to implement dual-band bandpass filter with narrow bandwidths. The fundamental even- and odd-mode frequencies are adopted to form first passband, and the harmonic ones construct the second passband. For dual-passband controllable, two pairs of loaded open stubs are employed, which only change the center frequency and external quality factor of the first passband. Thus, once the second passband has obtained the ideal frequency response, we can tune these two sets of stubs to achieve good impedance matching in the first passband. So the proposed filter will obtain low insertion loss and return loss in each passband. Moreover, transmission zeros are produced to improve the passband selectivity and band-to-band isolation due to source-load coupling. Finally, a practical dual-band filter with good performance is designed and fabricated. The measured results validate the proposed design.

2. ANALYSIS OF THE PROPOSED DUAL-BAND BPF

Figure 1(a) shows the geometrical schematic of the proposed dual-mode dual-band BPF. The SEDMR is based on a meander loop, which is divided into four equal parts by four points P_i ($i = 1, \ldots, 4$), as shown in Fig. 1(a), point P_1 is short circuited, and a short-stub loaded at point P_3 functions as a perturbation. In order to control the center frequency and external quality factor of the first passband, two pairs of open stubs, inside and outside of the loop, are loaded at points P_2 and P_4.

The composite transmission line model of the proposed dual-band BPF is illustrated in Fig. 1(b), which is composed of two branches

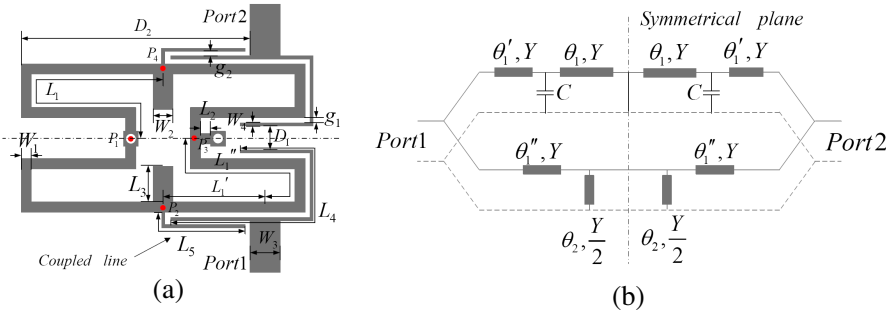

Figure 1. (a) Schematic of the proposed dual-band BPF. (b) Composite transmission line model.

in parallel, the upper one and the lower one. The loop and the perturbation have the same characteristic admittance Y, and the two pairs of loaded open-stubs can be equivalent to C. In order to maintain the symmetry of the circuit, the perturbation is divided into two parts with the same characteristic admittance $Y/2$. In addition, θ_i represents the electrical length of the corresponding transmission line.

The circuit model in Fig. 1(b) can be analyzed using even-odd-mode analysis. The even-mode circuit can be achieved by adding a magnetic wall along the symmetrical plane, therefore the input admittance Y_{in_even} from Port 1 is derived as follows:

$$Y_{in\_even} = Y_{1\_even} + Y_{2\_even} \tag{1a}$$

where

$$Y_{1\_even} = Y\frac{Y'_{1\_even} + jY\tan\theta'_1}{Y + jY'_{1\_even}\tan\theta'_1} \tag{1b}$$

$$Y'_{1\_even} = j\omega C - j\frac{Y}{\tan\theta_1} \tag{1c}$$

$$Y_{2\_even} = jY\frac{2\tan\theta''_1\tan\theta_2 - 1}{2\tan\theta_2 + \tan\theta''_1} \tag{1d}$$

$$\theta_1 = \theta'_1 + \theta''_1 \tag{1e}$$

The odd-mode circuit is modeled as an electric wall added along the symmetrical plane which can be seen as a short circuit. Its input admittance Y_{in_odd} from Port 1 is deduced as (2a)–(2c):

$$Y_{in\_odd} = Y_{1\_odd} + Y_{2\_odd} \tag{2a}$$

$$Y_{1\_odd} = Y_{1\_even} \tag{2b}$$

$$Y_{2\_odd} = -j\frac{Y}{\tan\theta''_1} \tag{2c}$$

It should be mentioned that (1a)–(1e) and (2a)–(2c) show that the electrical length θ_2 of the perturbation affects the even-mode frequency but has no relationship with the odd-mode one. When $L_3 = L_5 = 0$, Y_{in_odd} can be deduced from (2a)–(2c) that

$$Y_{in\_odd} = -jY \frac{\tan(2\theta_1)\left[1 - \tan\theta_1'' \tan\left(\theta_1 + \theta_1'\right)\right]}{\tan\theta_1'' \tan\left(\theta_1 + \theta_1'\right)} \tag{3}$$

According to the resonant condition $\mathrm{Im}\left(Y_{in\_odd}\right) = 0$, the odd-mode frequency can be given as follows

$$f_{odd} = \frac{n \cdot c}{4L_1\sqrt{\varepsilon_e}}, \quad n = 1, 2, 3 \ldots \tag{4}$$

where c is the velocity of light in free space, and ε_{eff} denotes the effective permittivity.

It is observed from (4) that the perimeter of the loop is a full wavelength at the fundamental odd-mode frequency, and the ratio of the harmonic odd-mode frequency when $n = 2$ to the fundamental one when $n = 1$ is 2.

As shown in Fig. 2, the two poles in each passband correspond to the fundamental and harmonic even- and odd-mode frequencies, respectively. The odd-mode frequency located at 1.87 GHz in the first passband is almost half the odd-mode frequency located at 3.58 GHz in the second passband, and the even-mode frequencies vary with the length L_2, while the odd-mode frequencies retain unchanged, which is in accordance with the above analysis. Thus, the length L_2 determines

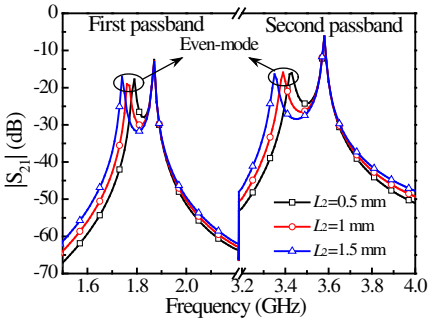

Figure 2. Simulated loose coupling transmission responses with different L_2 when $L_3 = L_5 = 0$.

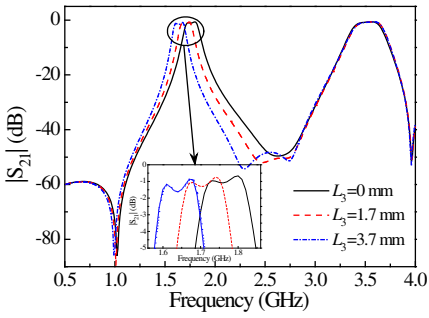

Figure 3. Simulated transmission responses against the length L_3. (Other dimensions of the structure are the same as those in Section 3).

the coupling strengths between even- and odd-mode in both passbands simultaneously, which leads to both passband bandwidths dependent of each other and will degenerate the filter property. What's worse, the center frequency ratio of the first and second passband is approximate 0.5 by nature. In order to solve the above problems, two pairs of open-stubs are introduced.

2.1. A Pairs of Open-stubs Inside of the Loop

In order to locate the center frequencies of the two passbands at the desired values, a pair of open-stubs inside of the loop loaded at points P_2 and P_4 is introduced. Fig. 3 illustrates the variation of simulated transmission responses with the length L_3 of the open-stubs, when keeping the length $L_5 = 0$. It is observed that the length L_3 increases from 0 to 3.7 mm, the first passband center frequency decreases from 1.763 to 1.64 GHz, while there is no influence on the second passband, which can be explained as follow.

Figure 4 gives the even- and odd-mode equivalence circuits and their voltage distributions, for a narrow bandwidth, the length L_2 of the perturbation is so small that the distance Δd between the voltage peaks of the fundamental even- and odd-mode or the voltage nulls of the harmonic even- and odd-mode is a small quantity, thus, the open-stubs loaded at points P_2 and P_4 almost can be neglected at both the harmonic even- and odd-mode frequencies, which form the second passband, however, will change the first passband center frequency constituted by the fundamental even- and odd-mode frequencies.

Therefore, the center frequencies of both passbands can be

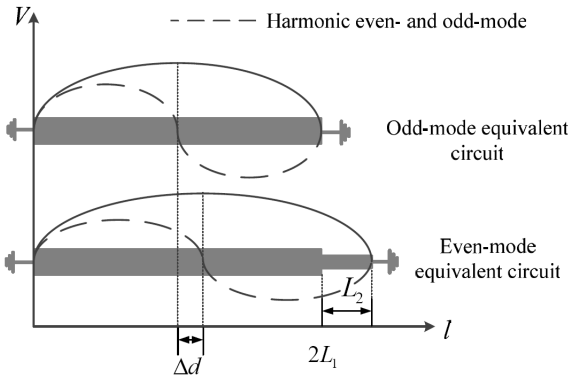

Figure 4. Even- and odd-mode equivalent circuits and their voltage distributions.

controllable in some extent after introducing this pair of loaded open-stubs. In addition, the loaded open-stubs also make attribute to the filter miniaturization, because the first passband center frequency shifts down.

2.2. Another Pairs of Open-stubs Outside of the Loop

The length L_2 of the perturbation determines the intercoupling strength in both passband simultaneously as the above analysis describes, in which nothing can be done. However, the external quality factor is another important parameter in filter design, and it can be tuned to match the fixed intercoupling strength.

Another pair of open-stubs outside of the loop (named as coupled line) with the length L_5 is adopted as shown in Fig. 1(a), and they have little influence on the second passband of interest as the above analysis states. Fig. 5 illustrates the simulated results of the filter with and without the coupled lines. After introducing the coupled lines, the first passband obtains an ideal response, while the second passband almost keeps unchanged. The even- and odd-mode external quality factors may be obtained via the simulation by placing a magnetic or electric wall along the symmetric plane of the excited resonator, respectively. Table 1 gives the extracted external quality factors in each passband of the proposed filter with and without the coupled lines. It is observed that the coupled lines bring more influence on the first passband than the second passband.

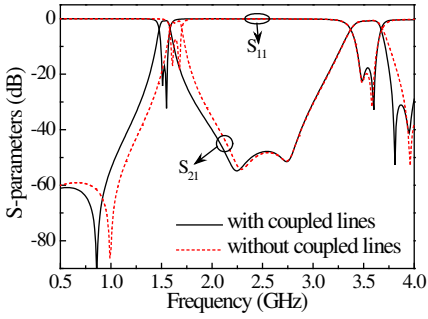

Figure 5. Simulated results of the proposed filter with and without coupled lines. (Dimensions of the structure are the same as those in Section 3).

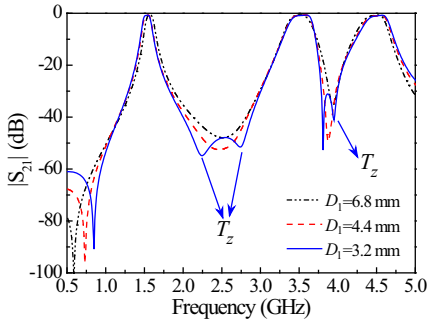

Figure 6. Simulated transmission responses of the proposed filter with different distance D_1.

In addition, the pair of loaded open-stubs outside of the loop will also decrease the first passband center frequency, and all the two pairs of open-stubs shift down it from the 1.763 to 1.52 GHz that we are interested in.

2.3. Source-load Coupling

In order to enhance the passband selectivity and band-to-band isolation, source-load coupling is introduced in this structure. Fig. 6 demonstrates the variation of transmission responses of the proposed filter against distance D_1. When the distance between two coupling sections of feed lines decreases, source-load coupling strength gets enhanced, and two new transmission zeros between the first and second passbands as the blue (solid) line depicts are generated to improve the passband selectivity and band-to-band isolation. Meanwhile, another new transmission zero located at 3.95 GHz is introduced too. Moreover, other transmission zeros move close to passband edges and enhance the passband selectivity.

3. FILTER DESIGN, FABRICATION AND MEASUREMENT

In this section, a novel dual-mode dual-band BPF will be designed based on the above analysis, and the design specifications are listed in Table 2. Due to the bandwidth of both passbands is not independent, the fractional bandwidth (FBW) of the first passband is not given.

Table 1. Extracted external quality factors with and without coupled lines.

Band / Q / State	Passband 1		Passband 2	
	Q_{even}	Q_{odd}	Q_{even}	Q_{odd}
With	22.94	23.1	22.72	30.7
Without	29.96	30.69	21.53	26.56

Table 2. Design specifications of the proposed filter.

	f_0/GHz	Return loss	FBW
Passband 1	1.52	18 dB	—
Passband 2	3.5	18 dB	7%

Table 3. The extracted return losses in the first passband under different lengths L_3 and L_5, when keeping the center frequency fixed at 1.5 GHz unchanged.

L_3 (mm)	3.6	3.7	3.8	3.9	4.0
L_5 (mm)	9.65	9.35	9.05	8.75	8.45
Return loss (dB)	19.6	18	17	16.2	15.6

According to filter synthesis in [23], the $[N+2]$ ideal practical coupling matrix of the second passband can be obtained as (5).

$$M = \begin{bmatrix} 0 & M_{Se} & M_{So} & 0 \\ M_{Se} & M_{ee} & 0 & M_{Le} \\ M_{So} & 0 & M_{oo} & M_{Lo} \\ 0 & M_{Le} & M_{Lo} & 0 \end{bmatrix} = \begin{bmatrix} 0 & 0.0568 & -0.0568 & 0 \\ 0.0568 & -0.1047 & 0 & 0.0568 \\ -0.0568 & 0 & 0.1047 & 0.0568 \\ 0 & 0.0568 & 0.0568 & 0 \end{bmatrix} \tag{5}$$

where the subscripts S, L, o and e represent source, load, odd-mode and even-mode, respectively.

The even- and odd-mode frequencies of the second passband are calculated by the diagonal elements in the coupling matrix, and their relationship is

$$M_{ii} = \left(f_0^2 - f_i^2\right) / \left(\Delta f \cdot f_i\right) \tag{6}$$

Here, the parameters f_0 and Δf are the center frequency and the bandwidth of the second passband, respectively.

According to (6), the even- and odd-mode frequencies of the second passband are 3.4872 and 3.5128 GHz, respectively. And then, the perimeter $4L_1$ of the meander loop can be computed by the Equation (4) with $n = 2$. Once the length L_1 is fixed, tuning the length L_2 to obtain the even-mode frequency of the second passband, meanwhile, the even- and odd-mode frequencies of the first passband have also been determined. And then, the length L_4 and g_1 must be confirmed for the coupling coefficients M_{Se} and M_{So} in (5). Finally, two pairs of open-stubs must be added to achieve the center frequency and proper external quality factors of the first passband. Table 3 lists the extracted return losses in the first passband under different lengths L_3 and L_5 via the simulation, while keeping the center frequency fixed at 1.5 GHz unchanged. It is observed that the lengths L_3 and L_5 have an inverse relationship if the first passband center frequency remains constant, and the return loss will increase when the length

L_5 decreases. Thus, a reasonable combination of L_3 and L_5 should be choose according to the design specifications of first passband.

Simulation is carried out using Zeland IE3D software, and the demonstration filter is designed on the substrate with a relative dielectric constant of 2.65 and thickness of 1 mm. The finally optimal geometric dimensions are given in Fig. 7, and the inset is the photograph of the fabricated filter. The measurement is implemented by Agilent's 8719ES network analyzer. Fig. 7 shows the comparison of the simulated and measured results. There is some discrepancy between them due to unexpected tolerance in fabrication and implementation. The measured two passbands are centered at 1.51 and 3.47 GHz with 3 dB fractional bandwidth of 5.9% and 6.9%.

Table 4. Performance comparison between the proposed filter and other techniques.

Ref.	Number of resonators	Circuit Area ($\lambda_g \times \lambda_g$)	$\lvert S_{21}\rvert$ (dB)	Isolation (dB)
[5]	4	0.25×0.15	2/2.5	23
[14]	2	0.43×0.21	2.46/2.89	50
[16]	2	0.23×0.23	3.5/4.8	22
[18]	1	0.31×0.31	1.1/1.6	45
[20]	1	0.4×0.3	3/2.5	28
This work	1	0.21×0.13	1.47/0.95	50

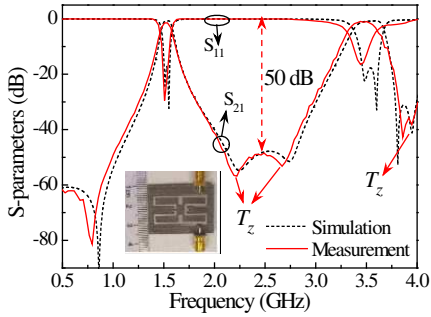

Figure 7. The simulated and measured results of the proposed filter. (The inset shows a photograph of the fabricated filter). ($L_1 = 30.2$ mm, $L_2 = W_1 = 1$ mm, $L_3 = 3.7$ mm, $L_4 = 16.5$ mm, $L_5 = 9.35$ mm, $L_6 = 7.8$ mm, $W_2 = 2$ mm, $W_3 = 2.9$ mm, $W_4 = 0.3$ mm, $g_1 = g_2 = 0.2$ mm, $D_1 = 3.2$ mm, $D_2 = 22.7$ mm).

The measured insertion losses are 1.47 and 0.95 dB at the center frequencies. Three new transmission zeros located at 2.19, 2.67 and 3.96 GHz introduced by the source-load coupling improve the passband selectivity and band-to-band isolation better than 50 dB. The overall circuit size is $0.21\lambda_g \times 0.13\lambda_g$, where λ_g is guide wavelength of the first passband. In final, Table 4 is provided to compare the proposed filter with those in [5, 14, 16, 18, 20] in terms of a few key parameters. It is observed that the proposed filter in this paper occupies smaller size and exhibits better performance in passband and higher band-to-band isolation.

4. CONCLUSION

In this paper, a novel dual-mode dual-band BPF based on SEDMR is proposed. Two pairs of open-stubs are employed to control the first passband center frequency and external quality factor, which forms a dual passband controllable dual-band BPF. Moreover, these loaded open-stubs shift down the first passband center frequency and miniaturize the filter circuit size in some extent. Transmissions zeros introduced by source-load coupling enhance the passband selectivity and improve the band-to-band isolation better than 50 dB. In this filter design, the procedure is simple and the loaded two pairs of open-stubs increase the design freedom degrees, so this proposed filter will be attractive in the wireless communication systems.

ACKNOWLEDGMENT

This work was supported by the National High Technology Research and Development Program of China (863 Program) No. 2012AA01A308 and the National Natural Science Foundation of China (NSFC) under Project Nos. 61271017 and 61072017.

REFERENCES

1. Hong, J. S. and M. J. Lancaster, *Microstrip Filters for RF/Microwave Applications*, Wiley, New York, 2001.
2. Wolff, I., "Microstrip bandpass filter using degenerate modes of a microstrip ring resonator," *Electron. Lett.*, Vol. 8, No. 12, 302–303, Jun. 1972.
3. Wu, B., C.-H. Liang, Q. Li, and P.-Y. Qin, "Novel dual-band filter incorporating defected SIR and microstrip SIR," *IEEE Microw. Wireless Compon. Lett.*, Vol. 18, No. 6, 392–394, Jun. 2008.

4. Dai, G.-L., Y.-X. Guo, and M.-Y. Xia, "Dual-band bandpass filter using parallel short-ended feed scheme," *IEEE Microw. Wireless Compon. Lett.*, Vol. 20, No. 6, 325–327, Jun. 2010.
5. Xue, W., C.-H. Liang, X. W. Dai, and J. W. Fan, "Design of miniature planar dual-band filter with 0° feed structures," *Progress In Electromagnetics Research*, Vol. 77, 493–499, 2007.
6. Velázquez-Ahumada, M. D. C., J. Martel-Villagr, F. Medina, and F. Mesa, "Application of stub loaded folded stepped impedance resonators to dual-band filter design," *Progress In Electromagnetics Research*, Vol. 102, 107–124, 2010.
7. Ma, D., Z.-Y. Xiao, L. Xiang, X. Wu, C. Huang, and X. Kuo, "Compact dual-band bandpass filter using folded SIR with two stubs for WLAN," *Progress In Electromagnetics Research*, Vol. 117, 357–364, 2011.
8. Wu, G.-L., W. Mu, X-W. Dai, and Y.-C. Jiao, "Design of novel dual-band bandpass filter with microstrip meander-loop resonator and CSRR DGS," *Progress In Electromagnetics Research*, Vol. 78, 17–24, 2008.
9. Kuo, J.-T. and S.-W. Lai, "New dual-band bandpass filter with wide upper rejection band," *Progress In Electromagnetics Research*, Vol. 123, 371–384, 2012.
10. Kuo, J.-T., S.-C. Tang and S.-H. Lin, "Quasi-elliptic function bandpass filter with upper stopband extension and high rejection level using cross-coupled stepped-impedance resonators," *Progress In Electromagnetics Research*, Vol. 114, 395–405, 2011.
11. Mondal, P. and M. K. Mandal, "Design of dual-band bandpass filters using stub-loaded open-loop resonators," *IEEE Trans. Microw. Theory Tech.*, Vol. 56, No. 1, 150–155, Jan. 2008.
12. Zhang, X. Y., J.-X. Chen, Q. Xue, and S.-M. Li, "Dual-band bandpass filters using stub-loaded resonators," *IEEE Microw. Wireless Compon. Lett.*, Vol. 17, No. 8, 583–585, Aug. 2007.
13. Chen, Z.-X., X.-W. Dai, and C.-H. Liang, "Novel dual-mode dual-band bandpass filter using double square-loop structure," *Progress In Electromagnetics Research*, Vol. 77, 409–416, 2007.
14. Fu, S., B. Wu, J. Chen, S.-J. Sun, and C.-H. Liang, "Novel second-order dual-mode dual-band filters using capacitance loaded square loop resonator," *IEEE Trans. Microw. Theory Tech.*, Vol. 60, No. 3, 477–483, Mar. 2012.
15. Zhang, X. Y. and Q. Xue, "Novel dual-mode dual-band filters using coplanar-waveguide-fed ring resonators," *IEEE Trans. Microw. Theory Tech.*, Vol. 55, No. 10, 2183–2190, Oct. 2007.

16. Chen, J.-X., T. Y. Yum, J.-L. Li, and Q. Xue, "Dual-mode dual-band bandpass filter using stacked-loop structure," *IEEE Microw. Wireless Compon. Lett.*, Vol. 16, No. 9, 502–504, Sep. 2006.
17. Luo, S. and L. Zhu, "A novel dual-mode dual-band bandpass filter based on a single ring resonator," *IEEE Microw. Wireless Compon. Lett.*, Vol. 19, No. 8, 49–499, Aug. 2009.
18. Sung, Y., "Dual-mode dual-band filter with band notch structures," *IEEE Microw. Wireless Compon. Lett.*, Vol. 20, No. 2, 73–75, Feb. 2010.
19. Li, Y. C., H. Wong, and Q. Xue, "Dual-mode dual-band bandpass filter based on a stub-loaded patch resonator," *IEEE Microw. Wireless Compon. Lett.*, Vol. 21, No. 10, 525–527, Oct. 2011.
20. Zhao, L.-P., X.-W. Dai, Z.-X. Chen, and C.-H. Liang, "Novel design of dual-mode dual-band bandpass filter with triangular resonators," *Progress In Electromagnetics Research*, Vol. 77, 417–424, 2007.
21. Chiou, Y.-C., P.-S. Yang, J.-T. Kuo, and C.-Y. Wu, "Transmission zero design graph for dual-mode dual-band filter with periodic stepped-impedance ring resonator," *Progress In Electromagnetics Research*, Vol. 108, 23–36, 2010.
22. Sun, S.-J., B. Wu, T. Su, K. Deng, and C.-H. Liang, "Wideband dual-mode microstrip filter using short-ended resonators with centrally loaded inductive stub," *IEEE Trans. Microw. Theory Tech.*, Vol. 60, No. 12, 3667–3673, Dec. 2012.
23. Cameron, R. J., "Advanced coupling matrix synthesis techniques for microwave filters," *IEEE Trans. Microw. Theory Tech.*, Vol. 51, No. 1, 1–10, Jan. 2003.